physica status solidi b

www.pss-b.com

Detecting Magnetic Permeability and Electrical Conductivity Fluctuations in Metallic Ferromagnetic Sheets through the Shielding Effect

Antonio Hernando, Fernando Giacomone, Jordi Viñolas, Miguel Angel García, Fernando Galvez, Alberto Castellanos, Alfonso de Hoyos, and Andres Cerracín*

In this report, a method is proposed for determining the fluctuations of physical and structural properties in metallic ferromagnetic samples by magnetic scanning. The method is based on the shielding of a circular loop electromagnetic field source using a ferromagnetic and metallic sheet. The shielding of the electromagnetic field depends on the field frequency and amplitude as well as the electrical conductivity and magnetic permeability of the sheet. The proposed method does not require winding around the sheet. The experimental AC shielding results are reported.

1. Introduction

Noninvasive techniques based on impedance changes have been developed for a long time using electromagnetic fields[1–4] to monitor the electromagnetic properties of samples. The impedance of an antenna or coil system depends on the frequency of the electromagnetic field, its electrical resistance, capacitance, and inductance. Such magnitudes are determined by a combination of the geometry and electromagnetic properties of the medium (electric conductivity and magnetic permeability). The large number of possible combinations of the involved physical parameters explains the broad adaptability of the method to different cases and accounts for the wide spectrum of applications in which impedance has been reported to be used as a sensing variable for some electromagnetic properties.

More complete studies related to the shielding of electromagnetic fields produced by coils parallel or perpendicular to a plane shield were carried out by Moser[5] and Bannister,[6,7] as summarized by Celozzi et al.[6] In particular, Celozzi et al.[6] indicated that the nonlinear magnetic behavior of ferromagnetic materials introduces distortion in the transmitted fields that drastically changes their harmonic contents.

In this study, the possibility of using the shielding strength produced by a metallic sheet for a rapid estimation of its conductivity and permeability fluctuations in ferromagnetic sheets was analyzed experimentally after an adequate approximation within the shielding standard theory was introduced.[5–8] The approximation considered and the experiments indicate that the method makes it possible to detect the fluctuations of the electromagnetic properties along the sheet surface used as a shielding material.

This study aimed to demonstrate the possibility of detecting fluctuations in the electromagnetic properties, such as magnetic permeability and electrical conductivity, of a metallic and ferromagnetic sheet by rapid measurement of its shielding coefficient—for instance, in railways to predict possible breaking

A. Hernando, F. Giacomone, A. Castellanos
Instituto de Magnetismo Aplicado
UCM-CSIC-ADIF
Las Rozas, P. O. Box 155, 28230 Madrid, Spain
E-mail: antherna@ucm.es

A. Hernando
Departamento de Física de Materiales
Universidad Complutense de Madrid
28040 Las Rozas, Spain

A. Hernando, J. Viñolas, A. de Hoyos
Universidad Antonio de Nebrija
calle de los Pirineos 55, 28040 Madrid, Spain

The ORCID identification number(s) for the author(s) of this article can be found under https://doi.org/10.1002/pssb.202100446.

DOI: 10.1002/pssb.202100446

A. Hernando
Imdea Nanociencia
C/Faraday 9, 28049 Madrid, Spain

A. Hernando
Donostia International Physics Center
Universidad del Pais Vasco
C/Manuel de Lardizabar 5, 20018 San Sebastián, Spain

M. A. García
Instituto de Cerámica y Vidrio (ICV) CSIC
Kelsen 5, 28049 Madrid, Spain

F. Galvez
Universidad de Castilla-La Mancha
13071 Toledo, Spain

A. Cerracín
Consultrans SAU
C/Agustín de Foxá 26, 28036 Madrid, Spain

by accumulative residual stresses. The method does not provide a precise determination of these properties, but rather a quick detection of their fluctuations that can originate from residual stress distribution, compositional fluctuations, fatigue, or recrystallization.

Initially, the theory of the ideal case of shielding of the magnetic field produced by a single circular coil is introduced. Second, the influence of frequency on the measurement and the general experimental conditions are discussed, keeping in mind the properties of the steel and carbon. Subsequently, experimental results are shown. The results obtained for the railway illustrate the sensitivity of the method to the electromagnetic property fluctuations. Finally, the conclusions are outlined briefly.

2. Theory

The theory applied to solve shielding problems has been based on three analytical techniques: 1) thin shield analysis; 2) transmission theory of shielding; and 3) exact solution of the wave equation.[5] Here, the last of these procedures is used.

A coil with radius r_0, carrying an AC current $I_0 e^{i\omega t}$. The coil is contained in the x–y-plane, parallel to the surface of a metallic ferromagnetic sheet of thickness d and at a distance h measured along the z-axis, as depicted in **Figure 1**. An attempt is made to determine the field at any point placed at the same distance d of the sheet, and at a distance r' from the coil axis, but on the opposite side, as shown in the figure. The dimensions of the sheet along the y-axis, Δy, are larger than r_0, whereas its length $\Delta x \to \infty$. When the distance $r^* = \sqrt{r_0^2 + (2h-d)^2}$ is less than the free space wavelength, the term associated with the displacement current or the propagation constant of air can be disregarded.[9] Therefore, the vector potential, A_Φ, verifies the Laplace equation, $\Delta A = 0$ or

$$\frac{\partial^2 A_\Phi}{\partial r^2} + \frac{1}{r}\frac{\partial A_\Phi}{\partial r} - \frac{A_\Phi}{r^2} + \frac{\partial^2 A_\Phi}{\partial z^2} = 0 \tag{1}$$

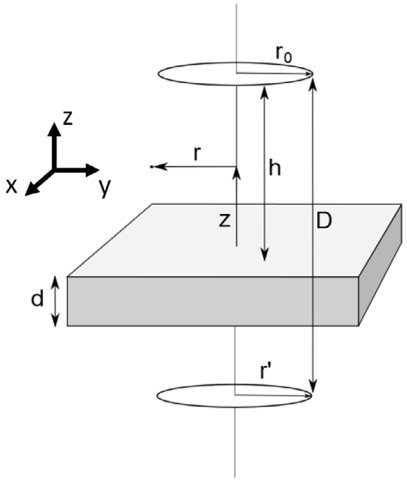

Figure 1. Scheme of primary and secondary coils with a metallic sheet in between and definition of geometrical parameters.

Here, A_Φ should contain only one term owing to the primary coil current, $A_{\Phi c}$, which becomes[9]

$$A_{\Phi c} = \frac{\mu_0 I_0 r_0}{2}\int_0^\infty e^{-k|z|} J_1(kr) J_1(kr_0)\mathrm{d}k \tag{2}$$

where the origin of the z-axis is taken at the center of the primary coil and $J_1(kr)$ is the corresponding Bessel function.

In the absence of the metallic sheet, the magnetic field component along the z-axis at the center of the pickup coil ($r = 0$) becomes[7]

$$\begin{aligned} B_{0z}(z = 2h + d, r = 0) = (\nabla x A_{\Phi c})_z &= \frac{\partial A_{\Phi c}}{\partial r} - \frac{1}{r^2} A_{\Phi c} \\ &= \frac{\mu_0 I_0}{2}\int_0^\infty k e^{-k|z|} J_1(kr_0)\mathrm{d}k \end{aligned} \tag{3}$$

After introducing the metallic sheet with relative magnetic permeability μ_r and electric conductivity σ, the vector potential is modified in the three regions: 1) $z < h$, 2) $h < z < h + d$, and 3) $z > h + d$. The new vector potential at each region can be expressed as follows:

In region 1, it becomes $A_{\Phi c} + A_{\Phi ec1} = A_{\Phi 1}$, where $A_{\Phi ec1}$ is the vector potential created by the eddy currents induced in the metallic sheet, and can be written as

$$A_{\Phi 1} = \frac{\mu_0 I_0 r_0}{2}\int_0^\infty (e^{-k|z|} + D_1(k) e^{kz}) J_1(kr) J_1(kr_0)\mathrm{d}k \tag{4}$$

Similarly, the potential vector in regions 2 and 3 can be expressed as

$$\begin{aligned} A_{\Phi 2} = \frac{\mu_0 \mu_r I_0 r_0}{2}\int_0^\infty &\left(D_2(k) e^{-\sqrt{k^2+\gamma^2}z} + D_3(k) e^{\sqrt{k^2+\gamma^2}z}\right) \\ &\times J_1(kr) J_1(kr_0)\mathrm{d}k \end{aligned} \tag{5}$$

$$A_{\Phi 3} = \frac{\mu_0 I_0 r_0}{2}\int_0^\infty D_4(k) e^{-kz} J_1(kr) J_1(kr_0)\mathrm{d}k \tag{6}$$

Inside the metallic ferromagnetic sheet, region 2, the vector potential verifies, instead of Equation (1), the following Poisson equation:

$$\frac{\partial^2 A_\Phi}{\partial r^2} + \frac{1}{r}\frac{\partial A_\Phi}{\partial r} - \frac{A_\Phi}{r^2} + \frac{\partial^2 A_\Phi}{\partial z^2} = -\mu j_\Phi \tag{7}$$

where μ is the magnetic permeability of the sheet and j_Φ holds for the eddy current density. Therefore, $j_\Phi = i\omega\sigma A_\Phi$, where σ is the conductivity of the sheet.

The solutions of Equation (7) have the form of sums over k of either $A(k) I_1(kr) e^{\pm ikz}$ or $A(k) J_1(kr) e^{\pm\sqrt{k^2+\gamma^2}z}$, with $\gamma = \sqrt{i\omega\sigma\mu_0\mu_r}$ and a corresponding skin depth, $\delta = \sqrt{\frac{2}{\omega\sigma\mu_0\mu_r}}$. To make it easier to include the boundary condition, the second type of solution is considered.

Equation (5) makes it possible to infer the eddy current density j_Φ as $-\sigma\frac{\partial A_{\Phi 2}}{\partial t}$.

The correct expressions of the four different $D_i(k)$ functions can be found from the boundary conditions at $z = h$ and

$z = h + d$, which corresponds to the continuity of A_Φ, at $z = h$, $A_\Phi(z = h^+) = A_\Phi(z = h^-)$, and, at $z = h + d$, $A_\Phi(z = (h + d)^+) = A_\Phi(z = (h + d)^-)$, as well as the continuity of the tangential component of the magnetic field H. This last condition implies conservation at $z = h$ and $z = h + d$ of

$$H_{\mathrm{ri}} = \frac{1}{\mu_0 \mu_r} \frac{\partial A_{\phi \mathrm{i}}}{\partial z} \tag{8}$$

By solving these algebraic systems of the four variables D_i, the following value is obtained for the constant included in $A_{\Phi 3}$:

$$D_4 = 4C \frac{\sqrt{k^2+^2}}{k} \mu_r e^{-d\left(\sqrt{k^2+\gamma^2}-k\right)} \tag{9}$$

where C verifies the following relation

$$C = \left[\left(\frac{\sqrt{k^2+\gamma^2}}{k} + \mu_r \right)^2 - \left(\frac{\sqrt{k^2+\gamma^2}}{k} - \mu_r \right)^2 e^{-2d\sqrt{k^2+\gamma^2}} \right]^{-1} \tag{10}$$

After introducing the metallic sheet, the z-component of the magnetic field along the coil axis is

$$B_z(z = 2h + d, r = 0) = \frac{\partial A_{\Phi 3}}{\partial r} - \frac{1}{r^2} A_{\Phi 3} \tag{11}$$

According to Equation (6), (9), and (11), $B_z(z = 2h + d, r = 0)$ becomes

$$B_z(z = 2h + d, r = 0) = 2\mu_0 \mu_r I_0 r_0 \int_0^\infty C\sqrt{k^2+\gamma^2} J_1(kr_0) \times e^{-k2h-d\left(\sqrt{k^2+\gamma^2}-k\right)} \mathrm{d}k \tag{12}$$

Therefore, the ratio between the fields observed at the center of the pickup coil before and after the introduction of the metallic sheet achieves an index of the shielding effectiveness. According to Equation (3) and (12), such a ratio is given by

$$\frac{B_{0z}}{B_z} = \frac{1}{4\mu_r} \frac{\int_0^\infty k e^{-2hk} J_1(kr_0)\mathrm{d}k}{\int_0^\infty C\sqrt{k^2+\gamma^2} J_1(kr_0) e^{-2hk} e^{-d}\mathrm{d}k} \tag{13}$$

2.1. DC Shielding

For a DC current flowing through the primary or source coil $\gamma = 0$, Equation (10) leads Equation (13) to become

$$\frac{B_{0z}}{B_z} = \frac{1}{4\mu_r} \frac{\int_0^\infty k e^{-2hk} J_1(kr_0)\mathrm{d}k}{\int_0^\infty [(1+\mu_r)^2 - (1-\mu_r)^2 e^{-2dk}]^{-1} k e^{-2hk} J_1(kr_0)\mathrm{d}k} \cong \frac{(1+\mu_r)^2}{4\mu_r} \tag{14}$$

where the term $(1 - \mu_r)^2 e^{-2dk}$ has been neglected with respect to the term $(1 + \mu_r)^2$. Such an approximation is stronger as d becomes larger than 2 h.

Here, $\int_0^\infty k e^{-2hk} J_1(kr_0)\mathrm{d}k = \frac{{r_0}^2}{(r_0^2+4h^2)^{\frac{3}{2}}}$, which, by considering Equation (3), yields $B_{0z}(z = 2h + d, r = 0)$, in agreement with the magnetostatic field produced by a current loop along its axis.

It is important to remark that DC shielding measurements using ferromagnetic sheets show the nonlinearity of the magnetization curve, that is, the magnetic susceptibility depends on the applied field. The theory is found on the basis of constant permeability that in the case of a ferromagnet implies a constant frequency and applied field. Therefore, in this case, the analysis of the relation between experimental results and this theory should be attempted under constant frequency and applied field strength conditions. Bannister[7] has shown some measurements of shielding by steel sheets as well as its comparison with theory.

2.2. AC Shielding (Low Frequency, that is, $\omega = 2\pi\nu < 10^5\ \mathrm{s}^{-1}$ or $\lambda > 10^4$ m)

For this frequency range, the vacuum wavelength is larger than 10 km, and the displacement current is negligible, as assumed in the theoretical development previously indicated. However, for a sheet thickness, d, of 0.015 m, relative permeability $\mu_r = 50$, (this value is apparently rather low but it is justified by shape geometry, that reduces the effective relative permeability along the not-easy directions, and by the relative high frequency of the field[10]), and conductivity of $5 \times 10^6\ (\Omega \cdot \mathrm{m})^{-1}$, which is typical of carbon steel, the skin depth of the sheet for $\nu = 1000$ Hz becomes $\delta = 0.0027$ m. The distance between any point of the loop and the measuring point is given by

$$r^* = \sqrt{r_0^2 + (2h - d)^2} = 0.0616\ \mathrm{m} \tag{15}$$

where the following values have been considered $r_0 = 0.02$ m, $h = 0.035$ m, and $d = 0.012$ m. The ratio $\frac{r^*}{\delta} \approx 11$.

When $\frac{r^*}{\delta} > 10$, Bannister[5,7] has shown that the propagation constant inside the metallic sheet $\sqrt{k^2+\gamma^2}$ can be considered to be γ; therefore, C is then given by

$$C = \left[\left(\frac{\gamma}{k} + \mu_r \right)^2 - \left(\frac{\gamma}{k} - \mu_r \right)^2 e^{-2d\gamma} \right]^{-1} \tag{16}$$

where $\gamma = \sqrt{i\omega\sigma\mu_0\mu_r} = \frac{1+i}{\sqrt{2}}\sqrt{\omega\sigma\mu_0\mu_r} = \frac{1+i}{\delta}$.

The value of C can be approximated to simpler expressions for the two opposite conditions: 1) for nonmagnetic metallic sheets, the condition $|\gamma| \gg k\mu_r$ is often achieved, where the maximum relevant k is on the order of $\frac{1}{r}$; and 2) for a metallic magnetic shield, in general, it is verified that $k\mu_r > |\gamma|$. Under this last condition, the term $C\sqrt{k^2+\gamma^2} \cong C\gamma$ becomes

$$C\gamma \cong \frac{\gamma}{{\mu_r}^2} \tag{17}$$

and Equation (12) can then be rewritten as

$$B_z(z = 2h + d, r = 0) \cong \frac{2\mu_0 I_0 r_0 e^{-d}}{\mu_r} \int_0^\infty J_1(kr_0) e^{-k2h}\mathrm{d}k \tag{18}$$

For $2h > r_0$, the integral in Equation (18) can be expressed as

$$\int_0^\infty J_1(kr_0)e^{-k2h}\mathrm{d}k = \frac{r_0}{r^*(r^*+2h)} \tag{19}$$

Hence, B_z at the center of the pickup coil is

$$B_z(z=2h+d, r=0) \cong \frac{2\mu_0 I_0 r_0 \gamma e^{-\gamma d}}{\mu_r r^*(r^*+2h)} \tag{20}$$

It is worth to remark the independence of $B_z(z=2h+d, r=0)$ on the relative position of the sheet between the two coils is pointed out, provided that the distance between them, $d+2h$, remains constant. The calculations have been performed under the assumption that both coils are at the same distance, h, from either side of the sheet. If the coil system is translated a distance $\psi < h$ along the z axis, both coils are at distances $h+\psi$ and $h-\psi$, respectively. However, note that the field produced by the primary coil is attenuated through air a total distance h, independent of ψ, and a distance d through the metallic sheet. As a consequence of the exponential dependence depicted by expressions (2), (4), (5), and (6), the value of $B_z(z=2h+d, r=0)$ does not depend on ψ, as derived from Bannister calculations.[7]

This property is the more relevant one associated with the use of two coils, since it allows rapid measurements carried out by translating the coil system along the sheet. Note that possible small lateral displacements of the coil system with respect to the sheet, along the z-axis, become normally unavoidable. When only a coil is used, by measuring its self-inductance, any small translation along the z axis can induce changes in voltage larger than those originated by the electromagnetic properties fluctuation of the sheet.[5]

3. Experimental Results

For detecting fluctuations in the electromagnetic properties of the sheet, we induced an alternating magnetic field, B, by passing an AC current on the primary coil with frequency ω. The induced voltage at the secondary coil was given by

$$\begin{aligned} V &= i \cdot \omega \cdot \oint A_{\phi 3} \cdot r_0 \cdot \mathrm{d}\phi \\ &= i \cdot \omega \cdot \alpha \cdot B_z(z=2h+d, r=0)_z \end{aligned} \tag{21}$$

where $A_{\phi 3}$ is given by Equation (6), and α is a geometrical parameter, fixed by the dimensions of the coils and the distance between them. It was considered that radii of primary and secondary coils were equal to each other with the value r_0.

Any fluctuation of permeability and/or conductivity induced a fluctuation of the value given by Equation (21). Note that γ and μ_r changed when μ_r fluctuated and only γ when the conductivity fluctuated.

After substitution of B_z value given by Equation (20) in Equation (21), the relative change of the voltage induced by permeability, $\Delta\mu_r$, or conductivity, $\Delta\sigma$, fluctuations could be expressed as

$$\frac{\Delta V}{V} = \frac{\Delta B_z}{B_z} = \frac{\Delta\left(\frac{\gamma e^{(-\gamma d)}}{\mu_r}\right)}{\left(\frac{\gamma e^{(-\gamma d)}}{\mu_r}\right)} \tag{22}$$

Considering an increment $\Delta\mu_r$ (an identical procedure was valid for an increment of conductivity), the relative change of voltage obtained by derivation with respect to μr could be expressed at its first order and according to Equation (22) as

$$\Delta V = \Delta\left(\left(\frac{\gamma}{\mu_r}\right)\right) \cdot e^{(-\gamma d)} + \frac{\gamma}{\mu_r} \cdot \Delta(e^{(-\gamma d)}) \tag{23}$$

so

$$\frac{\Delta V}{V} = \frac{\Delta\left(\frac{\gamma}{\mu_r}\right)}{\left(\frac{\gamma}{\mu_r}\right)} + \frac{\Delta e^{(-\gamma d)}}{e^{(-\gamma d)}} \rightarrow \frac{\Delta V}{V} = \frac{\Delta\sqrt{\frac{\sigma}{\mu_r}}}{\sqrt{\frac{\sigma}{\mu_r}}} + \frac{\Delta e^{(-\gamma d)}}{e^{(-\gamma d)}} \tag{24}$$

Hence,

$$\frac{\Delta V}{V} = -\frac{1}{2}\frac{\Delta\mu_r}{\mu_r} - \psi\frac{\Delta\mu_r}{\sqrt{\mu_r}} \tag{25}$$

where ψ is the real component of $\sqrt{i\omega\sigma\mu_0 d^2}$.

Expression (25) illustrates the outstanding contribution of the exponential term that makes the relative increment of the voltage to be roughly one order of magnitude larger than that of μr provided that $\psi > 1$. Note, however, that for large values of ψ, the voltage decreased exponentially and the noise to signal ratio should also increase. Therefore, the optimal conditions were those for which ψ being large was compatible with the sensitivity of the measuring system. The contribution of the first term, in the last side of Equation (23), was one half of the relative change of μ_r and therefore was smaller than the exponential term contribution.

The experimental conditions were limited by the requirement that the induced voltage at the secondary coil must be detectable, a condition that, as outlined earlier, defined an appropriate frequency range of the applied field or primary current. To obtain a noticeable voltage, coils with many turns must be used. Consequently, the field and geometrical parameters consisted of a sum of terms such as those depicted in the theoretical model developed for a single-turn coil. Note that this mutual inductance parameter α should then enclose an n2 factor, n being the number of turns of the primary coil assumed to be equal to that of the secondary.

A coil with a length of 4 cm and a diameter of $2r_0 = 4$ cm, with its center located at a distance $h = 3.5$ cm from the sheet surface, was used as the primary coil. The sheet was a piece of commercial steel with the thickness of 1.2 cm, length of 50 cm, and height of 6 cm.

For an AC current, the induced voltage became a complex number according to Equation (20) and (21). This ratio could be experimentally obtained by measuring the complex voltage that could be determined (both, modulus, and phase) by using a lock-in amplifier. The phase difference between the primary current and the induced voltage was also measured by the lock-in by using a voltage proportional to the primary current as a reference. **Figure 2**a illustrates the modulus of the voltage induced in the pickup coil for different frequencies of the field produced by a constant AC primary current of 100 mA as a function of frequency. Figure 2b shows, at an adequate scale,

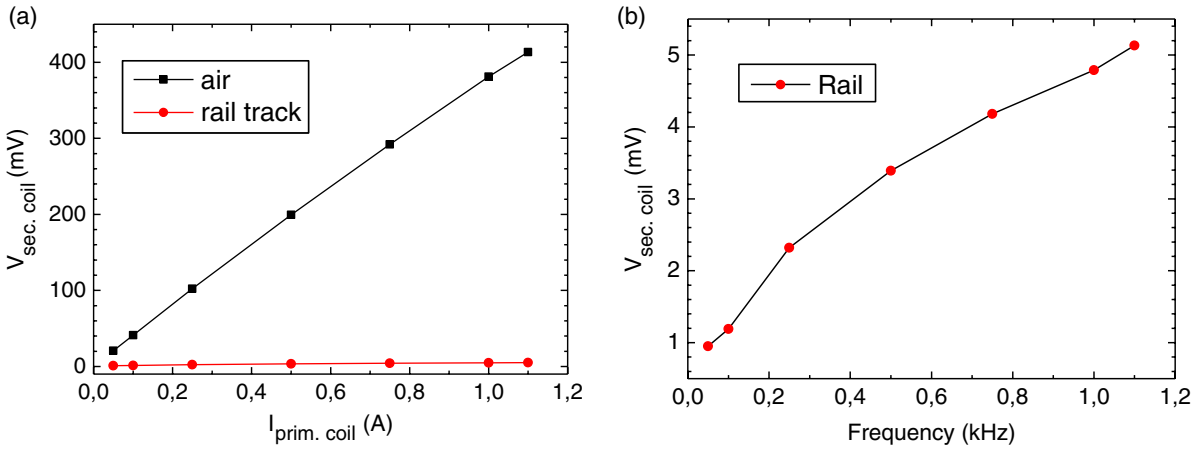

Figure 2. Pickup voltage detected with a lock-in amplifier at the secondary coil a) as a function of the current flowing along the primary coil at 1 kHz and b) as a function of frequency for an AC current of 100 mA flowing through the primary coil.

the dependence of the modulus of the induced voltage with the frequency when the sheet was intercalated between the primary and secondary coils. The lack of linearity was also associated with the ferromagnetic character of the sheet that yielded a dependence of the permeability with the frequency.

Concerning the optimum frequency, note that flux and induction increased with frequency, while penetration depth reduced. Hence, we found that optimum condition was a compromise in the range of kHz.

For detecting the fluctuations of either μ_r or σ, it was sufficient to measure the induced voltage for different positions. Therefore, by maintaining a constant intensity and frequency of the primary current and the distance between the primary coil and the point at which the field was measured, any change in the transmitted field and hence on the induced voltage should reflect a change in μ_r or σ.

4. Railway Measurements

The method was applied under real conditions in a 25 m-long railway. **Figure 3** shows picture of the experimental setup used to perform the measurements.

Figure 4 shows the results obtained by displaying the coil system along the railways using an AC current of 100 mA and a frequency of 1 kHz. It is important to confirm the high sensitivity of the method for detecting the periodic fluctuations of the electromagnetic properties of the rail associated with the periodic distribution of railroad ties. The induced voltage is plotted as a function of the position, indicating the measurements of ties and between the ties. The modification of the magnetic circuit introduced by the presence of ties strongly modifies the shielding capacity of the railway. The proximity to the dilatation meetings of the railway was also strongly detected.

The change in the rail magnetic anisotropy generated by internal stresses with values of the order of 200 MPa (about half of the elastic limit of the steel) is of $10^3\,\mathrm{Jm}^{-3}$, and provided a magnetostriction constant of 5×10^{-6}.[4] This change of anisotropy corresponds to a variation of approximately 5% of its average rail value that is also the expected order of the relative permeability change in those regions with internal stresses accumulation.[11] Therefore, these regions should be detectable through the changes in the induced voltage, as outlined later.

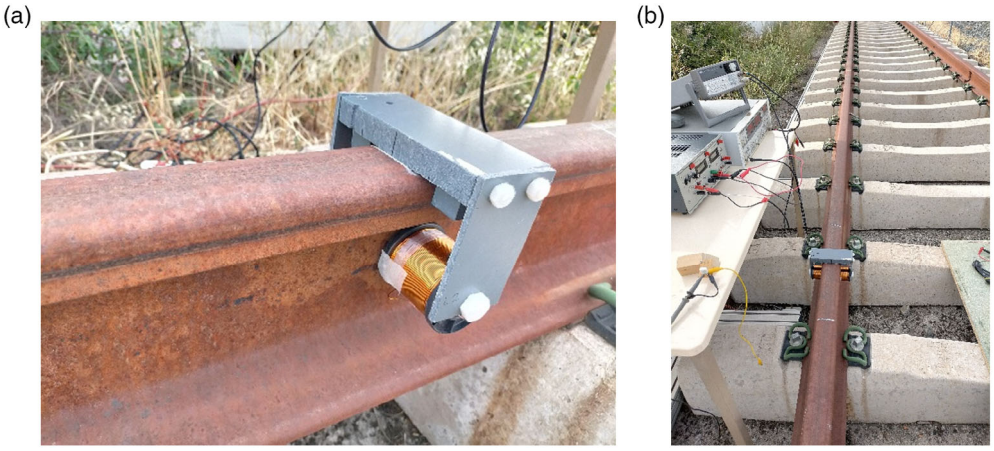

Figure 3. Pictures of a) the sensor head and b) the full setup to measure shielding when moving the sensor along the railway.

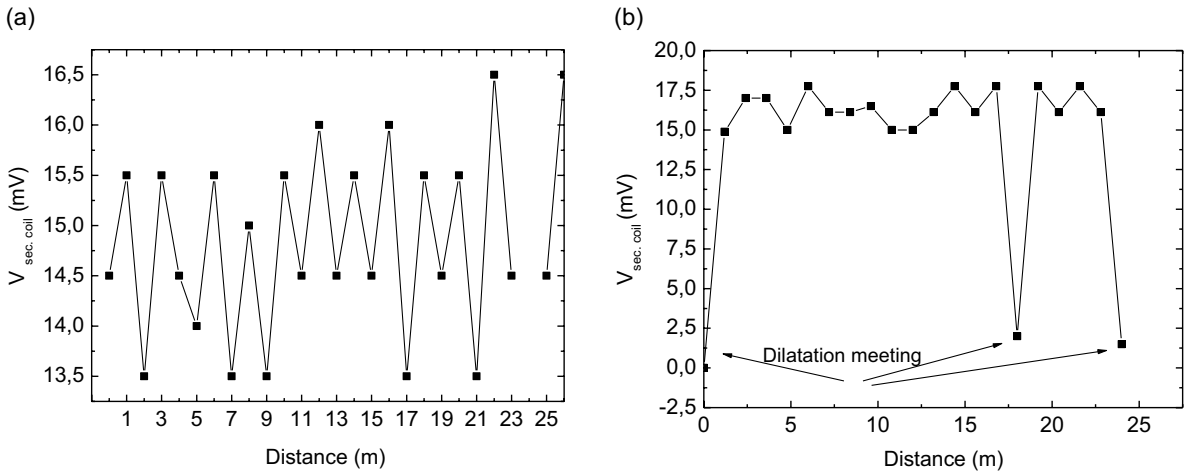

Figure 4. Fluctuations of the pickup voltage as a function of the position of the sensor when moving along a rail track.

When $|\gamma|d \approx 2.1\sqrt{\mu_r}$, the voltage fluctuation, induced by fluctuation of 5% in the value of μ_r (= 50), that is associated only with the exponential term in Equation (23), becomes

$$\frac{\Delta V}{V} = \frac{e^{-2.1\sqrt{52.5}} - e^{-2.1\sqrt{50}}}{e^{-2.1\sqrt{50}}} \approx 45\% \tag{26}$$

It has been considered $d = 0.015\,\text{m}$ and the value of $|\gamma|$ corresponding to $\omega = 2\pi \times 10^3$, $\sigma = 5 \times 10^6\,(\Omega\cdot\text{m})^{-1}$, and $\mu_0 = 4\pi \times 10^{-7}\text{Hm}^{-1}$. The large voltage fluctuation, as stated earlier, is a consequence of the exponential term that multiplies the permeability fluctuation by a factor 9.

Similar calculation performed at constant permeability and considering a 5% of conductivity fluctuations leads to an associated voltage fluctuation of 45% (the contribution of the first term in Equation (23) has been disregarded). These estimations illustrate the high sensitivity of the method to detect electromagnetic properties fluctuations. It is obvious that the same relative change of both properties should induce the same relative change of the exponential contribution. Note that on the base line defined by the sheet average properties, $\mu_r = 50$, $\sigma = 5\times10^6\,(\Omega\cdot\text{m})^{-1}$, and frequency of 1 kHz, it becomes obvious that any constant relative increment of either permeability or conductivity would increase in the same amount the term $|\gamma|d$ and consequently $\frac{\Delta V}{V}$.

5. Conclusions

The magnetic permeability and electrical conductivity of a metallic sheet govern its shielding capacity against electromagnetic fields. A rapid determination of the shielding effect produced by the sheet on the magnetic field generated by a coil provides some information about its magnetic and metallic character. The nonlinear behavior of ferromagnetic sheets is not a major drawback if both the intensity and the frequency of the field are maintained. From the calculations and experiments reported in this study, it can be concluded that, despite that the method is not suitable for precise measurement of the electromagnetic sheet properties, it provides some rapid and extremely high sensitive information about the fluctuation of these properties along the metallic tracks of railways. The rigid coil system can be displayed along the track travelling aboard of an auscultating train. Fluctuations in the voltage enable to detect fluctuations in composition, residual stresses, or microstructure.

Acknowledgements

This work was supported by the Spanish Ministerio de Ciencia, Innovación y Universidades through Research Project PID2020-114192RB-C41. F. Giacomone acknowledges grants PTA2015-10497-I and PTA2019-017584-I from Ministerio de Ciencia, Innovación y Universidades.

Conflict of Interest

The authors declare no conflict of interest.

Data Availability Statement

The data that support the findings of this study are available from the corresponding author upon reasonable request.

Keywords

electromagnetic properties, ferromagnetism, field propagation, steel

Received: August 30, 2021
Revised: February 24, 2022
Published online: March 21, 2022

[1] M. K. Devine, D. C. Jiles, A. R. Eichmann, D. A. Kaminski, S. Hardwick, *J. Appl. Phys.* **1993**, *73*, 5617.
[2] P. Vourna, A. Ktena, P. E. Tsakiridis, E. Hristoforou, *Measurement* **2015**, *71*, 31.
[3] A. P. Baghel, B. S. Ram, L. Daniel, S. V. Kulkarni, G. Krebs, J. B. Blumenfeld, L. Santandrea, *Comput. Mater. Sci.* **2019**, *166*, 96.

[4] M. S. García Alonso, A. Hernando, J. Viñolas, M. A. García, *J. Appl. Phys.* **2021**, *129*, 243901.
[5] J. R. Moser, *IEEE Trans. Electromagn. Compat.* **1967**, *EMC-9*, 6.
[6] S. Celozzi, R. Araneo, G. Lovat, *Electromagnetic Shielding*, John Wiley & Sons. Inc, Hoboken, NJ **2008**.
[7] P. R. Bannister, *IEEE Trans. Electromagn. Compat.* **1968**, *EMC-10*, 2.
[8] P. R. Bannister, *IEEE Trans. Electromagn. Compat.* **1968**, *EMC-11*, 50.
[9] W. K. H. Panofsky, M. Philips, *Classical Electricity and Magnetism*, Addison-Wesley, Reading, MA, **1962**, pp. 107–109.
[10] R. D. Cullity, *Introduction to Magnetic Materials*, Addison-Wesley, Boston, MA **1972**.
[11] E. Johnson, *Building Technology and Mechanics*, Report no. 2004 11, Boras, Sweden **2004**.